HEAT TRANSFER COMPARISON BETWEEN A VERTICAL RECTANGULAR CAVITY AND AN ISOSCELES RIGHT–ANGLED TRIANGULAR CAVITY OF EQUAL CROSS–SECTIONAL AREA

Antonio CAMPO*
Department of Mechanical Engineering,
The University of Texas at San Antonio,
San Antonio, TX 78239, USA

Jane Y. CHANG
Department of Applied Statistics
and Operations Research,
Bowling Green State University,
Bowling Green, OH 43403, USA

El Hassan RIDOUANE
Department of Mechanical Engineering,
The University of Vermont,
Burlington, VT 05405, USA

* Corresponding author: **campanto@yahoo.com**

Abstract

This paper addresses the heat transfer performance of natural convection flows in three different, (but related) cavities in the form of: a square, isosceles right-angled triangle, and vertical rectangle with aspect ratio 2:1. The isosceles right-angled triangular cavity is derived from a square cavity when cut in half diagonally, whereas the vertical rectangular cavity is derived from a square cavity when cut in half vertically. In the three cavities, the left vertical wall is the common wall heated. The buoyant air flow is characterized by height-based Rayleigh numbers ranging from a conduction-dominant to up to 10^6 for the laminar natural convection regime. Employing the finite volume method, the velocity and temperature fields as well as the mean convective coefficients evaluated at the common heated vertical wall are numerically determined for the isosceles right-angled triangular cavity. For this cavity, flow streamlines and temperature contours are presented in graphical form and some numerical results are validated against published experimental measurements. A one-to-one comparison for the heat transfer performance of the three interconnected cavities is reported in tabulated form.

Keywords: natural convection, laminar regime, square cavity, isosceles right-angled triangular cavity, 2:1 vertical rectangular cavity, heat transfer performance.

1. Introduction

A vast collection of studies encompassing theoretical analyses, numerical computations and experimental measurements for natural convection flows of single-phase fluids across two-dimensional stationary vertical, rectangular cavities has been disclosed in handbook chapters written by Raithby and Hollands [1], Charmchi and Martin [2] and Jaluria [3].

In particular, the specialized literature is superabundant with regards to natural convection in horizontal-placed right triangular cavities. In this configuration, there are two situations of interest: 1) a hot base, a cold inclined side and thermally insulated vertical side and 2) a cold base, a hot inclined side and thermally insulated vertical side. This topic is relevant to quantify the heat transfer characteristics of house and building attics within the framework of HVAC industries and representative publications are those of Asan and Namli [4], Haese and Teubner [5], Ridouane and Campo [6, 7] and some references cited therein. With regards to the results in [4, 5], it should be recognized that they are of limited utility because of the supposition that a plane of symmetry. This plane of symmetry exists for low flow and temperature values that correspond to low Rayleigh numbers. On the contrary, the flow and temperature results divulged in [6, 7] fully conform to the physics of the problem. Certainly, they are more accurate because the tricky idealization of the plane of symmetry was not invoked.

To the author's knowledge, the specialized literature is scarce for natural convection in vertical-placed right-angled triangular cavities. This specific layout of cavities finds application in contemporary electronic packaging because of space and/or weight constraints (Bar-Cohen et al. [8] and Simons et al. [9]).

In general, when buoyant fluid motion occurs in confined spaces like cavities, regardless of their shapes, the augmentation of natural convection heat transfer becomes a difficult task because of the low fluid velocities imparted by the acting gravitational forces. Owing to this adverse effect, it is of fundamental and practical interest to explore other suitable cavity shapes that promote the needed augmentation of natural convection in cavities. In general, the design engineer has to resort to experience, intuition and experimentation in order to improve the heat transfer performance of natural convection cavities. Thereby, the present paper is centered in studying the heat transfer performance of three cavities: the isosceles right-angled triangular cavity and the 2:1 vertical rectangular cavity; both are derived from the square cavity. The finite volume method is the vehicle used to determine the velocity and temperature fields induced by the buoyant air in the isosceles right-angled triangular cavity under the influence of low, moderate and large height-based Rayleigh numbers. Pertinent heat transfer information about the square and the 2:1 vertical rectangular cavities is taken from the specialized literature.

The body of the paper is divided into four sections. The first section describes the physical system and the mathematical formulation for the isosceles right-angled triangular cavity. The implementation of the finite volume method is explained in the second section. The third section contains the numerical-determined velocity and temperature fields as well as the total heat transfer rates through the heated vertical wall which is common to the three cavities. Finally, the comparison between numerical predictions and the available experimental measurements are included in the fourth section. In addition, for completeness this section contains a correlation equation needful for efficacious cavity design using air.

2. Physical system and mathematical formulation

A sketch of a stationary square cavity heated at the left vertical wall and cooled at the right vertical wall with the top and bottom walls being thermally insulated is unnecesary. In the context of natural convection cavities, Frederick [10] conducted a numerical study with air in several horizontal and vertical rectangular cavities with lateral heating/cooling at the two vertical walls. Selecting three different Rayleigh numbers for each aspect ratio Ar = H/W (H is the height and W is the base) comprised between 1 and 2, this author found that the heat transfer across the collection of cavities tested attained a maximum at different Rayleigh numbers. This discovery is equivalent to saying that such optimal cavity size lies between the square cavity and a vertical rectangular cavity twice the size of the square cavity. Motivated by the outcome of this work, to search for superior packaging, we decided to move further and explore two possibilities for cutting a square cavity in half in two different ways. Firstly, the square cavity was cut diagonally retaining the upper isosceles right-angled triangular cavity in Figure 1a with the diagonal wall cold. Secondly, the square cavity was cut vertically retaining the left vertical rectangular cavity in Fig. 1b owing an aspect ratio Ar = 2:1 with the right wall cold. While keeping the square cavity as the baseline case, the principal idea of the present study is to carry a parametric heat/fluid flow study of the two derived cavities sharing the same cross sectional area. In the three cases, the gravitational acceleration points downward. The dimension perpendicular to the plane of the trio of cavities is assumed to be long compared to other two dimensions, so that the laminar thermo-buoyant flow movement is predominantly two-dimensional. To avoid restrictions in the operational temperatures, the confined air is treated as a non-Boussinesqian fluid. Accordingly, the mathematical formulation written in Cartesian tensor notation (j = 1, 2) is:

Mass: $$\frac{\partial(\rho u_j)}{\partial x_j} = 0 \qquad (1)$$

Momentum: $$\rho u_j \frac{\partial u_i}{\partial x_j} = \frac{\partial}{\partial x_j}\left[\mu\left(\frac{\partial u_i}{\partial x_j} + \frac{\partial u_j}{\partial x_i}\right)\right] + X_i \qquad (2)$$

Energy: $$\rho c_p u_j \frac{\partial T}{\partial x_j} = \frac{\partial}{\partial x_j}\left(k \frac{\partial T}{\partial x_j}\right) \qquad (3)$$

Ideal gas equation of state: $p = \rho RT$ (4)

In eq. (2) X_i stands for the gravitational body force, being equal to $X_1 = 0$ in the horizontal direction and $X_2 = -g(\rho - \rho_{ref})$ in the vertical direction. Herein, the reference density ρ_{ref} is evaluated at a reference temperature $T_{ref} = (T_H + T_C)/2$.

The velocity boundary conditions are connected to: (a) solid, impermeable walls and (b) no slip air occurs at the bounding walls. For the temperature boundary conditions, a prescribed hot temperature at the left vertical walls, a prescribed cold temperature at the inclined wall and the right vertical walls in addition to the temperature gradient equal to zero at all horizontal wall(s).

The velocity and temperature fields of the circulatory air u (x, y), v (x, y), T (x, y) are obtained numerically. Based on the definition of the stream function ψ (x, y), the velocity field u (x, y), v (x, y) are post-processed first to determine the flow streamlines:

$$u = \frac{\partial \psi}{\partial y}, \quad v = -\frac{\partial \psi}{\partial x} \tag{5}$$

and the companion temperature contours. Second, the local wall heat flux q_w (y) is found by specifying Fourier's law at the hot vertical wall, (0, y), where the thermal conductivity k of the air is evaluated at the reference temperature $T_{ref} = (T_H + T_C)/2$. Third, the computation of the mean wall heat flux $\overline{q_w}$ is carried out by way of the mean value of the $q_w(y)$ function along the hot vertical wall:

$$\overline{q_w} = \frac{1}{H}\int_0^H q_w(y)\, dy \tag{6}$$

Fourth, the mean convective coefficient $\bar{h}$ on the hot vertical wall defined as

$$\bar{h} = \frac{\overline{q_w}}{(T_H - T_C)} \tag{7}$$

gives way to the equivalent mean Nusselt number

$$\overline{Nu}_H = \frac{\bar{h}\, H}{k} = \frac{\overline{q_w}}{(T_H - T_C)} \frac{H}{k} \tag{8}$$

3. Computational procedure

There is no need to redo the numerical calculations for the square cavity and the 2:1 rectangular cavity because there is a superabundance of heat transfer information for both in the specialized literature [1-3]. In view of this, the numerical computations are carried out for the isosceles right triangular cavity exclusively.

For a square and the 2:1 vertical rectangular cavities, the highly acclaimed correlation equation for the mean Nusselt number $\overline{Nu}_H$ developed by Berkosky and Polevikov [11] is

$$\overline{Nu}_H = 0.18\left[\left(\frac{Pr}{0.2+Pr}\right)Ra_H\right]^{0.29}\left(\frac{H}{W}\right)^{0.13} \quad \text{for} \begin{cases} 1<\dfrac{H}{W}<2 \\ 10^{-3}<Pr<10^{5} \\ Ra_H\left(\dfrac{Pr}{0.2+Pr}\right)\left(\dfrac{H}{W}\right)^{-3}>10^{3} \end{cases} \tag{9}$$

For the case of air or pure gases with Pr = 0.71, the above correlation equation simplifies to

$$\overline{Nu}_H = 0.17\,Ra_H^{0.29}\left(\frac{H}{W}\right)^{0.13} \quad \text{for} \begin{cases} 1<\dfrac{H}{W}<2 \\ Ra_H\left(\dfrac{H}{W}\right)^{-3}>1{,}282 \end{cases} \tag{10}$$

The numerical computations for the isosceles right-angled triangular cavity are performed with the finite volume code FLUENT 6.1 [12]. The computational domain being coincident with the physical domain was created and meshed with the grid generation software Gambit 2.0 ® [12]. In eqs. (1)–(4), the discretization of the convective term is accomplished by the second order accurate scheme QUICK, while the pressure-velocity coupling is handled with the SIMPLE scheme (Patankar [13].

As estimations for natural convection cavity flows are obtained at increasingly higher Rayleigh numbers, it is logical to question the physical reality behind the numerical solutions that are generated under the premises of laminar regime. Yet as the impressed wall-to-wall temperature difference (T_H – T_C) rises, all laminar convective flows become turbulent at sufficiently high Rayleigh numbers and many of them turn oscillatory over a certain range of Rayleigh numbers. The oscillatory regime usually is manifested somewhere in between the laminar and turbulent regimes. Le Quéré and Alziari de Roquefort [14] investigated the validity of steady solutions by way of analyzing laminar convective flows in a square cavity with top and bottom insulated walls. Using a time-dependent finite-difference code, these authors found that the onset of oscillations usually occurs at a Rayleigh number that ranges between 2 x 10^6 and 2.2 x 10^6. This solid recommendation will be adopted in this work too for one half of the square cavity. Basak et al. [15] analyzed the heat flow patterns in cavities using Bejan's heatline concept. The key parameters for our study are the Prandtl number, Rayleigh number and Nusselt number. The Rayleigh number has been varied from 10^2 to 10^5. For low Rayleigh number, it is found that the heatlines are smooth and perfectly normal to the isotherms indicating the dominance of conduction. But as *Ra* increases, flow slowly becomes convection dominant. It is also observed that multiple secondary circulations are formed for fluids with low *Pr* whereas these features are absent in higher *Pr* fluids. Multiple circulation cells for smaller *Pr* also correspond multiple cells of heatlines which illustrate less thermal transport from hot wall. On the other hand, the dense heatlines at bottom wall display enhanced heat transport for larger *Pr*.

Fixing T_H = 313 K and T_C = 287 K, the cavity height (the characteristic length) was varied to obtain different values of the Rayleigh number inside the interval (10^3, 10^6). Care was taken to increase the element density in vulnerable areas of the isosceles right-angled triangular cavity, such as near the solid walls where high velocity and temperature gradients would occur. Based on a sequence of numerical experiments, various grid sizes having between 30,000 up to 90,000 triangular elements were tried and examined. The optimal grid was found with 65,000 triangular elements carrying an error within 1%. This grid layout rendered ultra reliable results for the velocity and temperature fields u(x,y), v(x,y) and T(x,y) for all values of Ra_H. Also, global convergence was guaranteed by controlling the residuals of eqs. (1)–(4) to be less than 10^{-5}. After satisfactory convergence of the velocity and temperature fields was attained, we proceeded to calculate the streamlines, isotherms and mean wall heat flux at the vertical heated wall, $\overline{q}_w$. Needless to say, $\overline{q}_w$ is the ultimate quantity of interest for purposes of engineering analysis and design of cavities.

Experimental Validation

A search of the specialized literature revealed no experimental results for the size of the isosceles right-angled triangular cavity under study here. Luckily, experimental temperature measurements for a slender right-angled triangular cavity with apex angle α = 15° are available in Elicer-Cortés and Kim-Son [17]. Figure 2 illustrates a reasonable parity between the estimated and the measured air temperature profiles at three different relative heights y/H = 0.1, 0.58 and 0.99. The lowermost curve for y/H = 0.1 indicates that the numerical predictions overlap perfectly with the experimental measurements. From thermal physics, it may also be inferred that in this lower corner region, the air is basically remains motionless and the transfer of heat occurs by conduction. The numerical temperatures slightly overpredict the experimental observations at the other relative heights y/H = 0.58 and 0.99. The largest discrepancy occurs for the uppermost curve representative of the relative height y/H = 0.99. This location is very close to the horizontal insulated wall where the upward airflow slows down after turning the upper left corner but still moves horizontally with a vigorous velocity. Overall, the figure reaffirms that the agreement between the numerical and experimental temperatures of the air flows at the three locations is acceptable.

4. Discussion of Results

From the framework of thermal physics, knowledge of the departure from conduction and the onset of natural convection is of special interest. In the case of the isosceles right-angled triangular cavity, this phenomenon is quantified by an approximate critical Rayleigh number $Ra_{H,C} = 8\times10^3$, which is to roughly one order of magnitude higher than $Ra_{H,C} = 10^3$ for the counterpart square cavity.

When examining Figure 3, we observed contour plots of stream functions and temperatures for the isosceles right-angled triangle cavity characterized by a low $Ra_H = 10^3$. From the stream function plots, it can be seen that the configuration contains a single rotating vortex. The direction of the vortex rotation can be determined by finding the sign of the gradient for the stream function in the x-direction and also remembering that the velocity in the y-direction is opposite in sign to the stream function gradient. The vertical velocity is positive along the hot vertical wall and negative along the cold inclined wall and the vortex is rotating in a clockwise direction. Next, Figure 4 portrays the stream function and temperature contour plots for a high $Ra_H = 10^6$. In here, the presence of the strongest vortex is observable, which is in sharp contrast to the weak rotation strength illustrated in Figure 3. This specific vortex moves towards the zone with high horizontal thermal gradient (downwards) when Ra_H is increased.

Table 1 presents a comparison of the heat transfer performance for the three cavities under study, all influenced by various temperature differentials contained indirectly in the relative large Ra_H interval: $10^3 \leq Ra_H \leq 10^6$. The baseline case is obviously the square cavity. It is evident that for the natural convection effectiveness, the 2:1 vertical rectangular cavity outperforms the square cavity by a margin of approximately 17.5% for all $Ra_H < 10^6$. There is one exception for the low $Ra_H = 10^3$ where this margin descends to 9.52%. The superiority manifested by the isosceles right triangular cavity over the square cavity starts with a remarkable 235.71% at a low $Ra_H = 10^3$ and manifests a gradual decreasing behavior with increments in Ra_H. That is, the improvement is still high with 95.12% for $Ra_H = 10^4$ and for $Ra_H = 10^5$ comes down to 39.67%. This beneficial behavior can be explained in two parts. That is, 1) the stagnant core region in the isosceles right triangular cavity is smaller than in the 2:1 vertical rectangular cavity and 2) the ascending hot flow turns two 90° angles in the 2:1 vertical rectangular cavity whereas the flow turns one 90° degree angle and one 45° degree angle. Furthermore, a notable exception corresponds to the large $Ra_H = 10^6$ owing that the betterment is just 14.56%, as compared to 17.67% for the 2:1 vertical rectangular cavity.

A nonlinear regression analysis of the $\overline{Nu}_H$ vs. Ra_H data for the isosceles right triangular cavity was performed with Minitab [16]. The baseline involves the correlation equation for the square cavity

$$\overline{Nu}_H = 0.17\, Ra_H^{0.29} \tag{11a}$$

given in eq. (10). Correspondingly, two avenues are explored. A first outcome in additive form is

$$\overline{Nu}_H = 0.17\, Ra_H^{0.29} + 6.18 Ra_H^{-0.11} \tag{11b}$$

with R-square = 99.8% and maximum error 7.43% at Ra_H = 5,000. A second outcome in direct form is

$$\overline{Nu}_H = 4.54 + 18.6\left(\frac{Ra_H}{10^6}\right) - 12.8\left(\frac{Ra_H}{10^6}\right)^2 \tag{11c}$$

with R-square = 98.9% and maximum error 6.32% at Ra_H = 10,000. The two new correlation equations are valid for the moderate Ra_H-interval $10^3 \leq Ra_H \leq 10^6$.

When the magnitude of the mean Nusselt number $\overline{Nu}_H$ is known as a function of Ra_H, the heat transfer rate Q can be determined from "Newton's law of cooling":

$$Q = h\, A_S\, (T_H - T_C) = k\, \overline{Nu}_H\, A_S\, (T_H - T_C) \tag{12}$$

For the case of air with k = 0.026W/mC, the heat transfer rate per unit depth is

$$Q' = 0.026\, \overline{Nu}_H\, H\, (T_H - T_C) \tag{13}$$

where $\overline{Nu}_H$ is taken from either equation (11b) or (11c).

5. Conclusions

For the isosceles right-angled triangular cavity with a cold wall $\sqrt{2}\,H$ larger than the cold wall of the square and 2:1 vertical rectangular cavities relatively, it is evident that high fluid velocities exist. The heat transfer activity is higher in the bottom corner between the hot and cold walls, which occurs by conduction. In conclusion, it has been demonstrated that for purposes of heat transfer enhancement, the best is achieved by the isosceles right-angled triangular cavity up to $Ra_H = 10^6$ where both $\overline{Nu}_H$ equalize. From fluid physics, the onset of natural convection in the isosceles right-angled triangular cavity is dictated by $Ra_{H,C} = 8 \times 10^3$.

7. Acknowledgements

The authors ackwnowledge the suggestion by Dr. El Alami Semma from the Laboratoire de Mécanique, Université Hassan 1er, FST de Settat, Settat, Morocco.

Nomenclature

Ar	aspect ratio of cavity, H/W
A_S	surface area, [m^2]
c_p	specific heat at constant pressure, [J/ kg.K]
g	acceleration of gravity, [m/s^2]
Gr_H	Grashof number, $g\beta(\rho^2/\mu^2)(T_H - T_C)\, H^3$
$\overline{h}$	mean convective coefficient, [$W/m^2.K$]
H	height of cavity and characteristic length, [m]
k	thermal conductivity, [W/m.K]
$\overline{Nu}_H$	mean Nusselt number, $\overline{h}\, H/k$
p	pressure, [Pa]
Pr	Prandtl number, $\mu\, c_p/k$
q_w	wall heat flux, [W/m^2]
$\overline{q}_w$	mean wall heat flux, [W/m^2]
R	gas constant, [J/kg.K]
Ra_H	Rayleigh number, Gr_H Pr
T	temperature, [K]
T_C	cold wall temperature, [K]
T_H	hot wall temperature, [K]
T_{ref}	reference temperature, $(T_H + T_C)/2$, [K]
u, v	horizontal and vertical velocity components, [m/s]
U,V	dimensionless u, v
x, y	horizontal and vertical coordinates, [m]
X_i	gravitational body force, [kg/m^3]
X,Y	dimensionless x, y

W base of vertical rectangular cavity, [m]

Greek Letters

α apex angle formed between the vertical and inclined wall

β coefficient of volumetric thermal expansion, [1/K]

δ_{ij} Kroneker delta function

θ dimensionless temperature, $(T - T_C)/(T_H - T_C)$

μ viscosity, [kg/m.s]

ρ density, [kg/m^3]

ψ stream function, $u = \partial\psi / \partial y, \quad v = - \partial\psi / \partial x$

References

[1] Raithby, G. D., Hollands, K. G. T., "Natural Convection", Chapter 4, in Handbook of Heat Transfer, (Eds. W.M. Rohsenow et al.), 3rd. ed., Mc-Graw-Hill, New York, USA, 1998.

[2] Charmchi, M., Martin, J. G., "Natural Convection Heat Transfer", Chapter 3, in Handbook of Applied Thermal Design, (Ed. Guyer, E. C.), Taylor & Francis, Philadelphia, PA, USA, 1999.

[3] Jaluria, Y., "Natural Convection", Chapter 7, in Heat Transfer Handbook, (Eds. A. Bejan and A.D. Kraus), John Wiley, New York, USA, 2003.

[4] Asan, H., Namli, L., Laminar Natural Convection in a Pitched Roof of Triangular Cross Section: Summer Day Boundary Condition, *Energy and Buildings*, 33 (2000), pp. 69-73.

[5] Haese, P. M., Teubner, M. D., Heat Exchange in an Attic Space, *Intern. J. Heat Mass Transfer*, 45, (2002, pp. 4925-4936.

[6] Ridouane, E.H., Campo, A., Numerical Computation of Buoyant Airflows Confined to Attic Spaces under Opposing Hot and Cold Wall Conditions with Experimental Validation, *Intern. J. Thermal Sciences*, 44 (2005), pp. 944–952.

[7] Ridouane, E.H., Campo, A., Formation of a Pitchfork Bifurcation in Thermal Convection Flow Inside an Isosceles Triangular Cavity, Physics of Fluids, 8 (2006) 7, Paper number 074102.

[8] Bar–Cohen, A. et al., "Heat Transfer in Electronic Equipment", Chapter 13. In Heat Transfer Handbook, (Eds. A. Bejan and A.D. Kraus), John Wiley, New York, 2003.

[9] Simons, R. E., Antonnetti, V. W., Nakayawa, W., Oktay, S., “Heat Transfer in Electronic Packages”. In Microelectronics Packaging Handbook, (Eds. Tummala, R. R. et al.), 2nd. ed., pp. 1-315 to 1-403, Chapman and Hall, New York, USA, 1997.

[10] Frederick, R. L., On the Aspect Ratio for which the Heat Transfer in Differentially Heated Cavities is Maximum, *Intern. Comm. Heat Mass Transfer***,** 26 (1999) pp. 549-558.

[11] Berkosky, B.M., Polevikov, V.K., Numerical Study of High Intensive Free Convection. In *Heat Transfer and Turbulent Buoyant Convection*, (Eds. D.B. Spalding, N. Afgan), pp. 443-445, Hemisphere, Washington, DC,USA, 1977.

[12] www.fluent.com

[13] Patankar, S. V., Numerical Heat Transfer and Fluid Flow, Taylor & Francis Inc., New York USA, 1980.

[14] LeQuéré, P., Alziari de Roquefort, T., Transition to Unsteady Natural Convection of Air in Vertical Differentially Heated Cavities: Influence of Thermal Boundary Conditions on the Horizontal Walls, *Proceedings 8th Intern. Heat Transfer Conference*, San Francisco, CA, USA, 1986.

[15] Basak, T., Aravind, G., Roy, R., Visualization of Heat Flow due to Natural Convection Within Triangular Cavities using Bejan's Heatline Concept, *Intern. J. Heat Mass Transfer*, 52 (2009), 11-12, pp. 2824-2833.

[16] www.minitab.com

[17] Elicer-Cortés, J. C., Kim-Son, D., Natural Convection in a Dihedral Enclosure: Influence of the Angle and the Wall Temperatures on the Thermal Field, *Experimental Heat Transfer*, 6 (1993), pp. 205-213.

Table 1. Comparison of the heat transfer performance between a square cavity, the 2:1 vertical rectangular cavity and the isosceles right-angled triangular cavity

Ra_H	$\overline{Nu}_H$ square cavity Ref. [11]	$\overline{Nu}_H$ 2:1 vertical rectangular cavity Ref. [11]	% difference	$\overline{Nu}_H$ isosceles right-angled triangular cavity	% difference
10^3	1.26	1.38	9.52	4.23	235.71
5×10^3	2.01	2.36	17.41	4.35	116.42
10^4	2.46	2.89	17.48	4.80	95.12
5×10^4	3.92	4.61	17.60	5.95	51.79
10^5	4.79	5.64	17.75	6.69	39.67
5×10^5	7.64	8.99	17.67	9.13	19.50
10^6	9.34	10.99	17.67	10.70	14.56

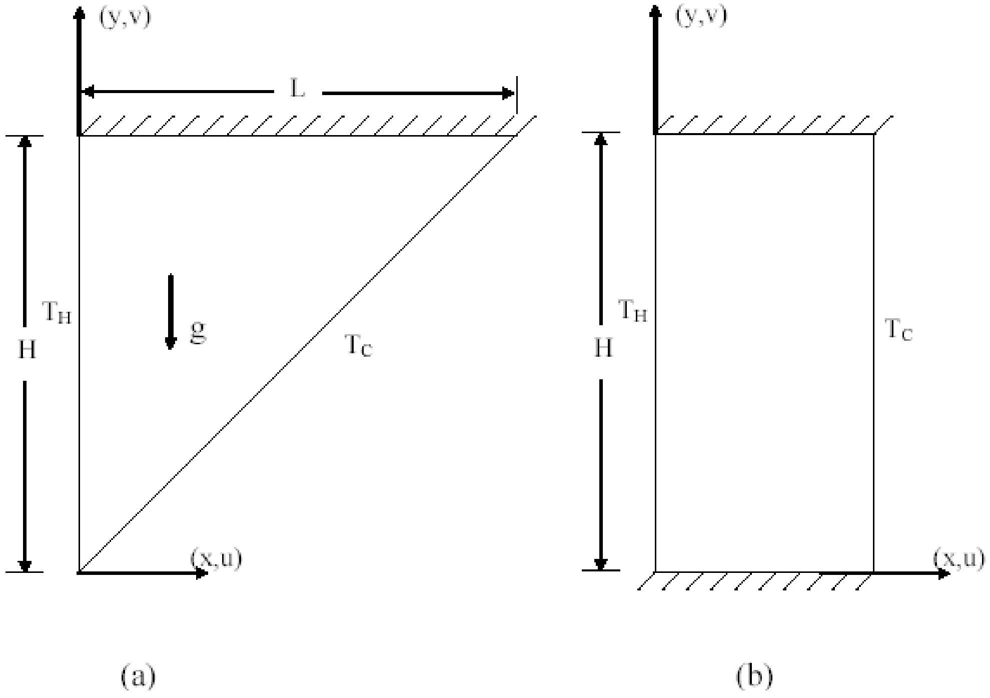

Figure 1 a) the isosceles right-angled triangular cavity, b) the 2:1 vertical rectangular cavity

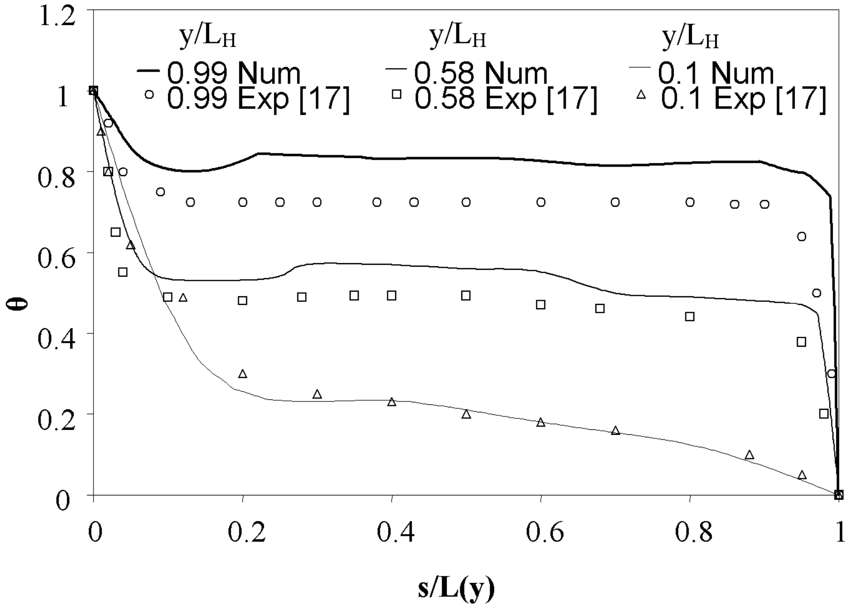

Figure 2 Comparison between the predicted and measured dimensionless temperatures in the isosceles right-angled triangular cavity

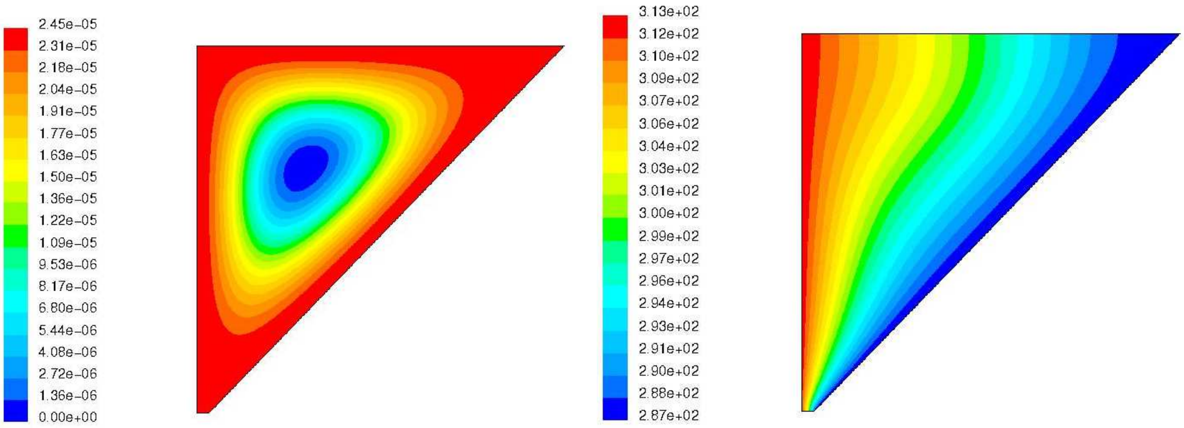

Figure 3. Stream functions and isotherms for an isosceles right-angled triangular cavity characterized by $Ra_H = 10^3$

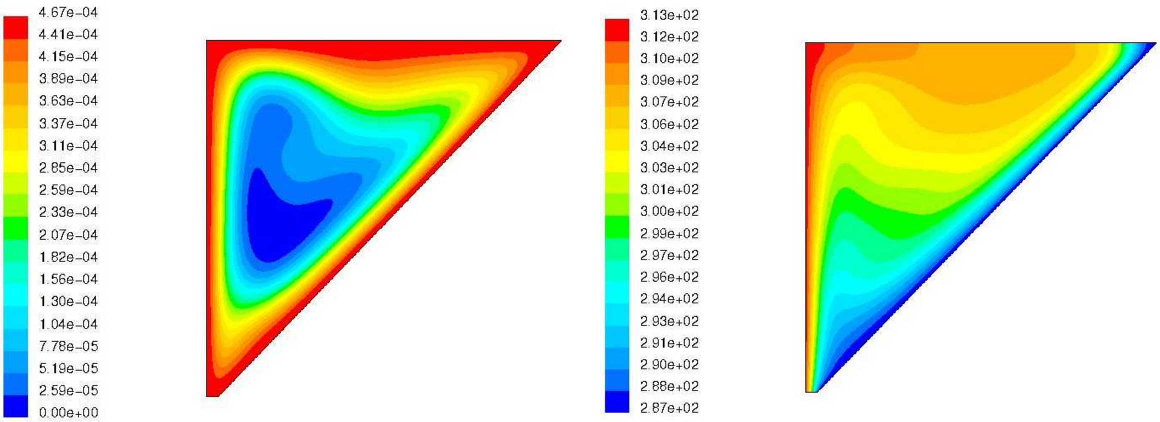

Figure 4. Stream functions and isotherms for an isosceles right-angled triangular cavity characterized by $Ra_H = 10^6$